Control Applications for Biomedical Engineering Systems

Edited by

Ahmad Taher Azar

Customized modeling and optimal control of superovulation stage in in vitro fertilization (IVF) treatment

13

Urmila Diwekar[a], *Apoorva Nisal*[b], *Kirti Yenkie*[c], *Vibha Bhalerao*[d]
[a]Vishwamitra Research Institute, Stochastic Research Technologies LLC, The University of Illinois at Chicago, Chicago, IL, United States, [b]The University of Illinois, Chicago, IL, United States, [c]Chemical Engineering, Rowan University, Glassboro, NJ, United States, [d]Jijamata Hospital and IVF Center, Nanded, India

1 Introduction

A survey conducted by the World Health Organization (WHO) in 2010 using data from 190 countries over a period of 20 years found that around 2% women suffer from primary infertility and 10% women suffer from secondary infertility. Primary infertility is the inability to conceive a first live birth and secondary infertility is the inability to conceive after a prior live birth. Certain regions of Eastern Europe, North Africa, Middle East, Oceania, and Sub Saharan Africa showed greater prevalence of infertility (Mascarenhas et al., 2012). In the United States itself, data collected by the Center for Disease Control (CDC) over a 4-year span showed 6.7% of married women to be suffering from infertility (FastStats, 2018).

In vitro fertilization (IVF) process is one of the most commonly recommended treatments in Assisted Reproductive Technologies (ART). 1.7% of infants were born through ART in the United States in 2015 (Sunderam et al., 2018). IVF is a process by which oocytes or egg cells are fertilized by a sperm outside the body in a laboratory simulating similar conditions in the body, and then the fertilized eggs or embryos are implanted back in the uterus for a full-term pregnancy. It has four basic stages (Fritz and Speroff, 2010): superovulation, egg retrieval, insemination/fertilization, and embryo transfer as shown in Fig. 1.

IVF is an expensive treatment, and the out-of-pocket costs per cycle tend to be around $10,000–$15,000. This cost varies and increases with multiple factors such as unsuccessful IVF cycles, multiple births, low-birthweight infants, and preterm births occurring from IVF cycles (Sunderam et al., 2018). The cost of IVF depends upon the cost of superovulation. Currently, this step is executed using almost daily monitoring of the follicular development using ultrasound and blood test. The daily dosage of hormones is customized for each patient based on these tests. Conventionally, doses are prescribed based on empirical data instead of randomized control trials

Control Applications for Biomedical Engineering Systems. https://doi.org/10.1016/B978-0-12-817461-6.00013-5
© 2020 Elsevier Inc. All rights reserved.

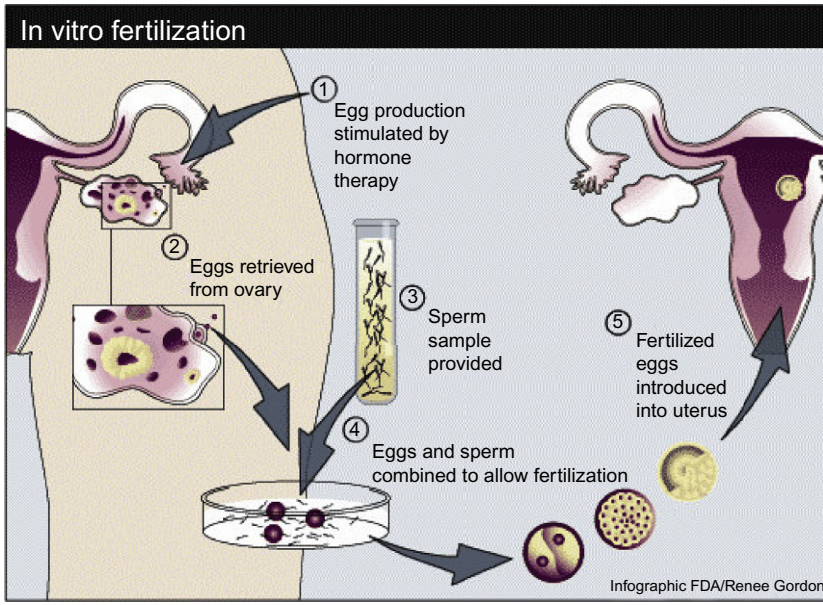

Fig. 1 Schematic diagram of the in vitro fertilization procedure (Gordon, 2012).
From Sage K. (2016) Reproductive Decisions. In: Child A. (eds) Diagnosis and Management of Marfan Syndrome. Springer, London.

and start at 150 or 225 IU. Devroey and team employed initial low-dose FSH (follicle-stimulating hormone) (100 IU) on a relatively young age group and recorded a high number of retrieved oocytes (Devroey et al., 1998). Prescribed minimum dosages start from 150 to 300 IU for younger patients and reach the absolute maximum at 450 IU for poor responders (Jungheim et al., 2015; Rombauts, 2007; Dorn, 2005). Certain factors, which come into play when choosing an FSH dose for a patient, are usually female age, anamnesis, clinical criteria, and ovarian markers such as AFC (antral follicle count) and AMH (anti-Mullerian hormone) (La Marca and Sunkara, 2014). FSH starting dose based on AFC was found to be less than 225 IU for most patients under the age of 35 years (La Marca et al., 2013). Although there are general guidelines for the dosage limits, the dose is not optimized for each patient. IVF procedure can have side effects such as the ovarian hyper stimulation syndrome (OHSS) (Alper et al., 2009), and the remedial actions are still unidentified. Around 1%–2% of women undergoing IVF suffer from a serious case of OHSS (Klemetti et al., 2005). Patients suffering from polycystic ovarian syndrome (PCOS) are found to be the ones most susceptible to OHSS. However, many patients who do not suffer from PCOS may also develop OHSS after stimulation. Protocols based on factors like age, AMH, AFC, FSH, BMI (body mass index) levels and smoking history predict optimal protocols with highest follicle yield and reduced occurrence of OHSS (Yovich et al., 2016). However, all the existing protocols are based on patient history, testing and monitoring, and professional judgment of the physician. The complications such as overstimulation or unsuccessful superovulation do occur. The cost associated with

patient monitoring and testing as well as the hormonal drugs make the superovulation stage very expensive. The evidence is building in support of personalized IVF treatment (Nyboe Andersen et al., 2017, Sighinolfi et al., 2017; Simopoulou et al., 2018) and tools that can suggest optimal patient-specific drug-dosage profiles to reduce hyperstimulation, cost of treatment, improve the oocyte quality, and quantity to increase the overall success rate of IVF, resulting in successful pregnancies and live birth. Trials have shown that mild stimulation individualized protocol for poor response patients with low antral follicular count (AFC < 11) yield similar pregnancy rates with largely reduced dosages per woman (van Tilborg et al., 2017; Youssef et al., 2016). A report evaluating merits of mild stimulation protocol for poor responders suggests that dosage of $\leq$150 IU/day yields high-quality oocytes and similar pregnancy rates compared to conventional protocols (Practice Committee of the American Society for Reproductive Medicine, 2018). A nomogram prediction model based on age, day 3 FSH and AMH to select appropriate starting FSH dose proposed by La Marca and team was validated through a randomized trial and showed an increased number of patients exhibiting optimal oocyte retrieval response (Allegra et al., 2017; La Marca et al., 2013). Moon and team also employed nomogram to predict the number of oocytes retrieved from IVF cycles from different univariate and multivariate models based on age, serum FSH, AFC, AMH levels (Moon et al., 2016). While both AFC and AMH are good predictors of ovarian reserve and oocyte yield, AFC poses advantages such noninvasive measurement, ease of testing, and smaller testing time over AMH (Fleming et al., 2015; Kotanidis et al., 2016). Recently, a modeling approach and a computerized algorithm to generate customized hormonal dosing policies for enhanced superovulation results, and reduced cost and decreased testing were presented by our group (Yenkie et al., 2013; Yenkie and Diwekar, 2014; Nisal et al., 2019). There are four commonly used protocols for IVF.

The four protocols (Scoccia, 2017), which are generally used: (1) Long Lupron agonist protocol, (2) microflare agonist protocol, (3) three-stop Lupron agonist protocol, and (4) Flexible GnRH antagonist (Ganerelix or Cetrorelix) protocol with NEA. This approach is presented for the first of the four protocols in this chapter. The validation of the procedure is carried out using clinical data from patients who have previously undergone IVF cycles. Initial two-day data for each patient are used to obtain parameters of the model for that patient. The model is used then to predict FSD for the remaining days of the cycle. This procedure was conducted for 49 patients. The results of the customized models are found to be closely matching with the observed FSD on the successive days of the IVF superovulation cycle. This customized model is then used to optimize the dosage for this patient. The FSD at the end of the cycle was determined using the model and the optimized dosages. A small clinical trial was also conducted in India. This was a double-blinded trial. The results show that the dosage predicted by using the model is 40% less than that suggested by the IVF doctors. It also shows that the number of mature follicles obtained at the end of the cycle using the dosage predicted by the model is significantly higher than that of physician suggested dosage. These results were consistent with all patients in this clinical trial. The testing requirements for these patients with optimized drug dosage are also reduced by 72%.

The rest of the chapter is arranged as follows. Section 2 describes the customized modeling approach for each patient, followed by Section 3 on the optimal control for the determination of hormonal dosage profiles for each patient. These two sections provide results for clinical data from 49 patient cycles obtained from Jijamata Hospital, Nanded, India. The overall approach is summarized in Section 4. This section also presents results from the small clinical trial conducted at the Jijamata hospital in India. Section 5 summarizes the overall approach and provides insights into our ongoing work and future directions.

2 Modeling of in vitro fertilization

In the superovulation stage of IVF, multiple follicles enter into the growth phase and increase in size due to externally injected hormones (Baird, 1987). There are significant similarities between the superovulation stage of IVF and the particulate process of batch crystallization (Hill, 2005; Yenkie and Diwekar, 2012), which has been well studied in the chemical engineering discipline. We used these similarities to develop a model for the daily follicle size distribution in IVF (Table 1).

The properties of a particulate system can be represented by moments of its particle size distribution (Randolph, 1988). The moment model for follicle number and size was adapted from the concept of batch crystallization (Hill, 2005) based on the analogy between batch crystallization and superovulation presented in Table 1. The superovulation follicle growth model, in general, resembles greatly to the growth of seeded batch crystals (Hu et al., 2005). The aim of seeded batch crystallization is to allow the seeds added to the solution to grow to desired shape and size and truncate the process of nucleation by maintaining certain process conditions. The numbers of seed added to the solution are constant and hence the zeroth moment of seeded batch crystals, which corresponds to its number, is constant. Similarly, when we look at superovulation, the

Table 1 Analogy between batch crystallization and IVF superovulation stage

Batch crystallization	**Superovulation (IVF stage I)**
• Production of multiple crystals	• Production of multiple oocytes or eggs
• Crystal quality is determined in terms of size distribution and purity	• Oocyte quality is determined in terms of no abnormalities, similar size
• The rate of crystallization or crystal growth varies with time and process conditions	• The rate of ovulation or oocyte growth varies with time and drug interactions
• The process is affected by external variables like agitation, and process operating variables like temperature, pressure, etc.	• The process is affected by externally administered drugs and body conditions of the patient undergoing the process

number of follicles activated during an IVF cycle is constant. Thus, the moment model for both the processes can be similar; the growth term, which is a function of process variables like temperature and supersaturation in seeded batch crystallization, becomes a function of hormonal dosage in case of superovulation process.

2.1 Data organization and moment calculation

Due to ovarian stimulation using externally injected hormones, the number of follicles entering the ovulation stage is more in number as compared to a single follicle in a normal menstrual cycle. The superovulation cycle data obtained from Jijamata Hospital, India, had measurements of follicle size and number along with the amounts of hormone administration. The data for example for patient 1 are reorganized as shown in Table 2 in terms of bin sizes of various diameters of follicles.

The data represented in Table 2 can be converted to moments using the general expression shown in Eq. (1).

$$\mu_i = \sum n_j(r,t) r_j^i \Delta r_j \tag{1}$$

Here, μ_i is the ith moment, $n_j(r,t)$ is the number of follicles in bin "j" of mean radius "r" at time "t," r_j is the mean radius of jth bin, and Δr is the range of radii variation in each bin. Here, the follicle sizes are divided into 6 bins; thus for efficient process modeling, it is essential to consider at least first 6 orders of moments along with the zeroth moment (Flood, 2002). Table 3 shows the moment values evaluated using Eq. (1).

2.2 Model equations

The moment-based model for predicting follicle size and number will involve the follicle growth rate and moment equations. It is assumed that the follicle growth is dependent on the amount of FSH administered since it the most influential hormone in

Table 2 Variation of follicle size (diameter) with time and FSH dose in patient

↓ Size bins (mm)	Number of follicles			
Time →	Day 1	Day 5	Day 7	Day 9
0–4	4	0	0	0
4–8	12	0	0	0
8–12	8	17	1	0
12–16	2	6	15	3
16–20	0	3	10	15
20–24	0	0	0	8
FSH dose (IU/ml)	150	75	75	75

IU—International units used for hormonal dosage measurement.

Table 3 Moments evaluated for patient 1

Sr. No	Time (day)	μ_0	μ_1	μ_2	μ_3	μ_4	μ_5	μ_6	FSH (IU/mL)
1.	1	52	188	820	4028	21556	123,068	738,100	150
2.	5	52	308	1924	12740	89428	662,228	5,131,684	75
3.	7	52	400	3140	25120	204500	1,691,440	14,189,540	75
4.	9	52	488	4660	45224	445492	4,449,128	44,994,100	75

follicular dynamics. Thus, the growth term is written as a function of FSH dose; as shown in Eq. (2). Here, G is the follicle growth term, k is the rate constant, ΔC_{fsh} is the amount of FSH injected, and α is the rate exponent.

$$G(t) = k\Delta C_{\text{fsh}}(t)^{\alpha} \tag{2}$$

The number of follicles activated for growth is assumed to be a constant due to the literature suggested by Baird (1987) and clinical data from the Jijamata hospital; hence, zeroth moment is constant. The 1st to 6th order moments are used for efficient recovery of the size distributions. The moment equations for the follicle dynamics are Eqs. (3)–(9). Here, $G(t)$ is the follicle growth term and μ_i is the ith moment. It can be clearly seen that the $(n + 1)$th moment is dependent upon the nth moment.

$$\mu_0 = \text{constant} \tag{3}$$

$$\frac{d\mu_1}{dt} = G(t)\mu_0(t) \tag{4}$$

$$\frac{d\mu_2}{dt} = 2G(t)\mu_1(t) \tag{5}$$

$$\frac{d\mu_3}{dt} = 3G(t)\mu_2(t) \tag{6}$$

$$\frac{d\mu_4}{dt} = 4G(t)\mu_3(t) \tag{7}$$

$$\frac{d\mu_5}{dt} = 5G(t)\mu_4(t) \tag{8}$$

$$\frac{d\mu_6}{dt} = 6G(t)\mu_5(t) \tag{9}$$

Patient parameters μ_0, k, and α for the models are determined from fitting the results of Eqs. (1)–(9) to the moment data at different times as shown in Table 2. In this protocol, in the clinical (experimental) settings, the attending physician determines the initial dosage for the patient based on various patient factors. The first-day ultrasound and blood test provides the baseline total number of follicles. The same dose is continued for the first four days and then testing with ultrasound and blood test starts. Depending on the tests, each day dose is determined based on the follicular distribution seen in ultrasound and the blood test results. Since there are three parameters involved, we need a minimum of two days of data for the model. The validity of the model can be evaluated by comparing the FSD predicted by the model from 5th day onwards with that of observed or experimental values.

2.3 FSD evaluation

Eqs. (2)–(9) predict the moment values. However, the desired output is required in the form of FSD; thus, the approach to obtain FSD from moment values is illustrated later. The distribution is approximated using the inversion matrix (**A**) shown in Table 4 along with a nonlinear constrained optimization technique (Flood, 2002; Yenkie et al., 2013). The method suggested is represented in Eq. (10), which can be rewritten to keep the unknown variable (n) on the L.H.S. as Eq. (12).

$$\mu = \mathbf{A}\, n \tag{10}$$

$$n = \mathbf{A}^{-1}\mu \tag{11}$$

Here, n is the vector of a number of follicles in all the size bins at the ith day in the cycle, μ is the moment vector for the ith day, and **A** is the inversion matrix. For the current bin size of 2 mm (radii) and the number of bins as 6, the inversion matrix **A** is shown in Table 4.

2.4 Follicle number prediction algorithm

To predict the number of follicles in a particular size bin on a particular day in the FSH dosage regime, a constrained optimization algorithm is applied. The optimization variables in the suggested algorithm are the number of follicles (n) per day in the superovulation cycle. Using this follicle number prediction algorithm, the moment model for follicle growth can be validated for a given patient.

Step #1: Assign some initial values for n (number of follicles/day) within the different size bins used in the model.
Step #2: Obtain the moment values by multiplying the matrix **A** with the initially assumed n values.
Step #3: Introduce the constraint for the total number of follicles. It is assumed that a constant number of follicles ($\mu_0/2$) enter the growth stage in the IVF cycle for a particular patient. Hence, for each day, the number of follicles must sum up to the assumed constant value.
Step #4: Restrict the values of n to be either positive or zero since the number of follicles can never be negative.

Table 4 The inversion matrix A (6 × 6) to recover size distribution from moments

A =	2	6	10	14	18	22
	2	18	50	98	162	242
	2	54	250	686	1458	2662
	2	162	1250	4802	13,122	29,282
	2	486	6250	33,614	118,098	322,102
	2	1458	31,250	235,298	1,062,882	3,543,122

Step #5: Write the objective function Eq. (12) to minimize the sum of the square of errors between the model predicted moments and the ones obtained from Eq. (10).

$$\text{Min } F(nk, j) = \sum_{i=1;j=1}^{i=m;j=N_{bins}} \left(\frac{\mu_{i,j}^{eval} - \mu_{i,j}^{model}}{\mu_{i,j}^{eval}} \right)^2 \tag{12}$$

Here, $n_{k,j}$ is the number of follicles on the kth day in j bins, i is the order of the moment (1–6), j is the number of bins, $\mu_{i,j}^{eval}$ is obtained by using Eq. (10), and $\mu_{i,j}^{model}$—obtained from moment model using optimum k and α.

Step #6: Use a constrained nonlinear optimization method to obtain the values of n.
Step #7: Compare the optimum values of n obtained from this constrained optimization method to the actual data observed for the patient.

2.5 Model validation

The model described here uses the data collected on the first and fifth days to calibrate the model. However, if all-day data are used, the model fit is going to be much better. Fig. 2 shows the FSD for various days observed in real practice (denoted as experimental values (E)) compared to the model predictions (denoted as (M)) considering data from considering all-day data (Fig. 2A) and considering only the two-day data (Fig. 2B) for patient 2. Similarly, the results are presented for patient 3 in Fig. 3A and 3B, respectively. This shows that the model performs very well for these two patients irrespective of either two-day or all-day data. The results of these two patients are selected as they represent two ends of the different age spectrum.

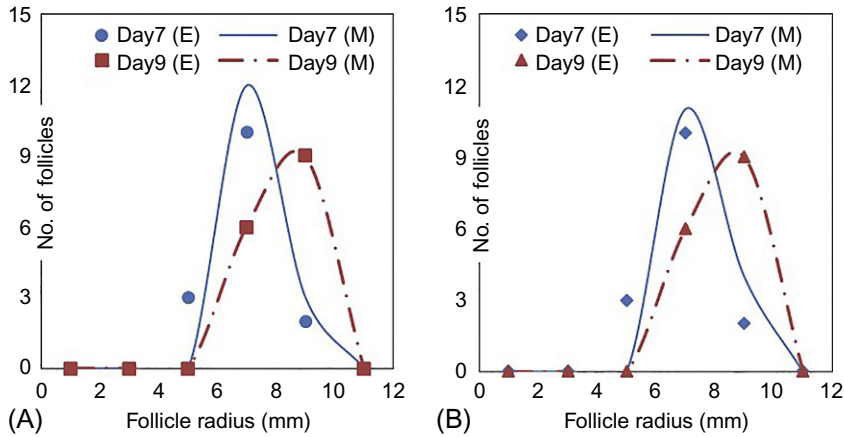

Fig. 2 Comparison of observed (E) follicular distribution with the follicle size distribution predicted by customized model (M) for various days for patient 2: (A) patient parameters estimated from all-day data and (B) patient parameters estimated using two-day data.

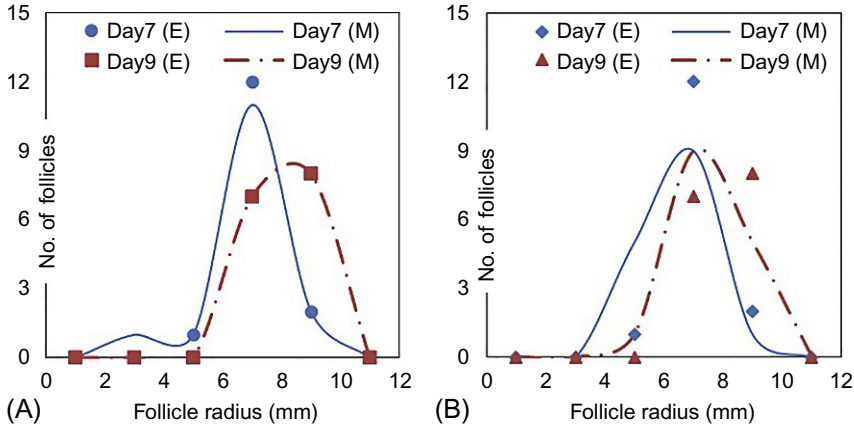

Fig. 3 Comparison of observed (E) follicular distribution with the follicular distribution predicted by customized model (M) for various days for patient 3: (A) patient parameters estimated from all-day data and (B) patient parameters estimated using two-day data.

As stated earlier, data have been gathered for 49 patients from Jijamata Hospital, India. The data are used to study the predictive capability of the model for the final day of stimulation. Fig. 4 presents the histogram of the ratio of final-day mature follicles predicted by the model ($n_{\text{mature, }M}$) to final-day mature follicles observed experimentally ($n_{\text{mature, }E}$) in real practice. Fig. 4A presents the prediction from all-day data and Fig. 4B presents predictions from the two-day data. For most of the patients (more than 90% of the patients), the model shows a good fit for all-day data versus 70%

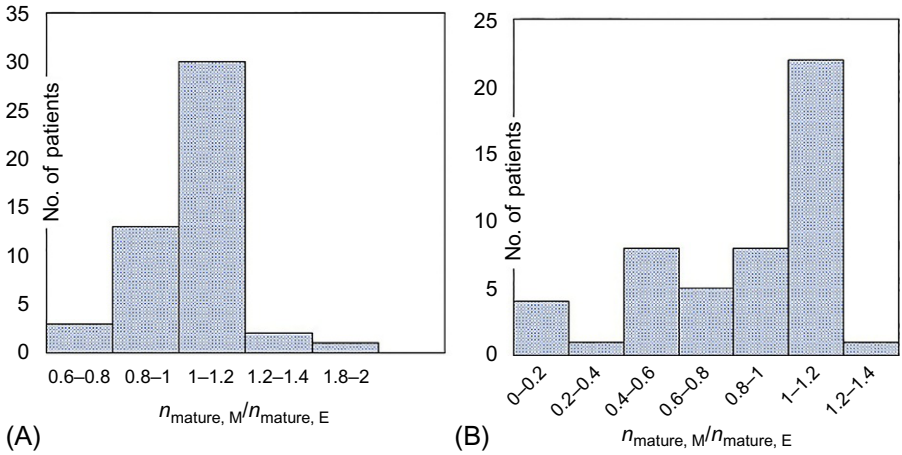

Fig. 4 Histogram of $n_{\text{mature},M}/n_{\text{mature},E}$ for 49 patients: (A) model fitted using all-day data and (B) model fitted using two-day data.

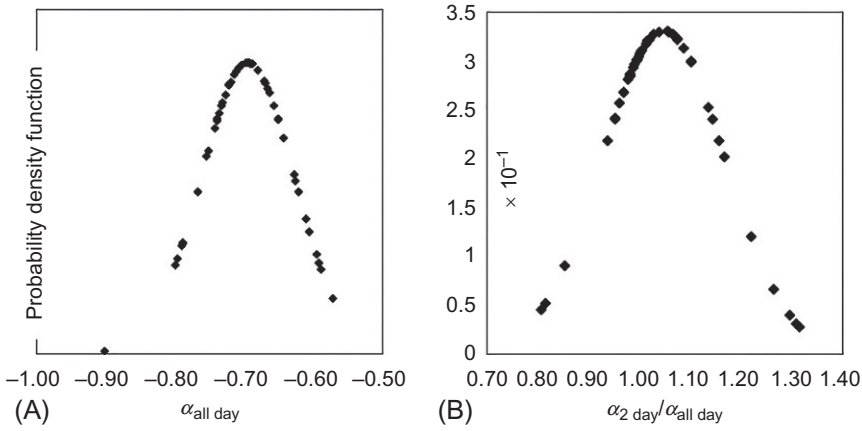

Fig. 5 Probability density function for the patient parameter α: (A) distribution of $\alpha_{\text{all-day}}$ and (B) distribution of error $\alpha_{\text{2-day}}/\alpha_{\text{all day}}$.

for two-day data predictions. Although the model predictions are not that good for 30% of the patients for the two-day data, it is important to find out whether the optimal control profile predicted using the 2-day data can be still used for these patients. This is studied in next section.

2.6 Results from parameter estimation

It has been observed that the model parameter k (follicle growth rate constant) is the same for all patients and is found to be 22. Therefore, it can be concluded that k is patient independent. However, α (follicle growth rate exponent) changes for each patient. The probability distribution for $\alpha_{\text{all-day}}$ and the distribution of error in $\alpha_{\text{2-day}}$ compared to $\alpha_{\text{all-day}}$ is shown in Fig. 5A and B, respectively. The analysis of the outliers from the histograms is presented in Fig. 4A. It is observed that two patients are outliers. Further analysis of these two patients revealed that $\alpha_{2\text{ day}}$ value for both is above -0.92. Thus, it can be said that the model is the best fit for values of alpha ranging from "-0.5" to "-0.9."

3 Optimal control for customized optimal dosage determination

Optimal control is a method for evaluating the time-varying values of certain process variables, also known as the control variable, which aid in achieving the desired outcome. It falls under a special category of optimization problems in which the optimization variable is a time-dependent vector instead of a single value. It has a wide range of applications in industrial processes, unit operations, and biomedicine.

In biomedical field, optimal control has been used for predicting cancer chemotherapy and tumor degradation (Castiglione and Piccoli, 2007; Czako et al., 2017), drug scheduling in HIV infection treatment (Khalili and Armaou, 2008), and for blood glucose regulation in insulin-dependent diabetes patients (Ulas Acikgoz and Diwekar, 2010).

There are various methods for solving optimal control problems such as calculus of variations, dynamic programming, maximum principle, and nonlinear programming discussed in detail by Diwekar (2008). In IVF, the control variable is the value of hormonal doses per day of the treatment cycle. The objective of superovulation is to obtain a high number (maximum possible) of uniformly sized (18- to 22-mm diameter) follicles on the last day of FSH administration.

3.1 Mathematical formulation

The data on superovulation cycles from the collaborators indicate that after the initial 4–5 days of FSH administration the follicle size and number plots tend to follow a Gaussian/Normal distribution and as time progresses this distribution continues to follow a Gaussian trend with a shift in the mean and variance. This distribution is used to define the objective function in terms of the moments. The moment model for FSD prediction and the method for deriving normal distribution parameters (John et al., 2007) have been used as the basis for deriving expressions for the mean and coefficient of variation.

Since the data clearly reflect a normal distribution, it is quite reasonable to assume it as an a priori distribution for follicles and the following mean (Eq. 13) and coefficient of variation (Eq. 14) expressions can be derived in terms of moments. Here, $\bar{x}$ is the mean follicle size, CV is the coefficient of variation.

$$\bar{x} = \frac{\mu_1}{\mu_0} \tag{13}$$

$$CV = \sqrt{\frac{\mu_2 \mu_0}{{\mu_1}^2} - 1} \tag{14}$$

Thus, the objective of superovulation in the mathematical form can be stated as to minimize the coefficient of variation on the last day of FSH administration ($CV(t_f)$) and the control variable shall be the dosage of FSH with time ($C_{fsh}(t)$). Here t_f is the final day of the cycle.

To customize the model for each patient, the parameters are evaluated using the initial two-day observations of the follicle size and counts along with the FSH administered. The optimal dosage prediction for the desired superovulation outcome is represented as Eq. (15).

$$\underset{C_{fsh}}{\text{Min}}\, CV(t_f) \tag{15}$$

Subject to:

(i) Follicle growth term and moment model
(ii) Additional equations for the coefficient of variation (CV) and mean ($\bar{x}$)

$$\frac{dCV}{dt} = \frac{G\mu_0}{C_v\mu_1}\left\{1 - \frac{\mu_0\mu_2}{{\mu_1}^2}\right\} \tag{16}$$

$$\frac{d\bar{x}}{dt} = G \tag{17}$$

(iii) The final size of the follicles must not exceed 22 mm in diameter.

3.2 Solution by maximum principle

The control problem has 9 state variables resulting in 9 state equations. For simplicity of notations "y_i" is used to denote the ith state variable. In maximum principle, one adjoint variable is introduced corresponding to each state variable. Thus, there are 9 adjoint variables resulting in 9 additional equations. Let z_i be the ith adjoint variable. The objective function is then converted to the Hamiltonian form (H), which on expansion involves the state as well as adjoint variables. The optimality condition for the problem is given by Eq. (22). A tolerance level is fixed for the derivative of the Hamiltonian with respect to the control variable (dH/dC_{fsh}) and can be written in a more realistic manner as the condition "$abs[dH/dC_{\mathrm{fsh}}|t] < tolerance$." Initial values are available for the state variables, whereas final values are available for the adjoint variables. This results in a two-point boundary value problem.

Let $y_i = [\mu_0\mu_1\mu_2\mu_3\mu_4\mu_5\mu_6 CV\bar{x}]$ then;

$$\mathrm{Max}_{C_{\mathrm{fsh}}(t)}\{-\mathrm{y}_8(t_\mathrm{f})\} \tag{18}$$

$$\frac{dy_i}{dt} = f(y_i, t, C_{\mathrm{fsh}}) \tag{19}$$

$$\frac{dz_i}{dt} = \sum_{j=1}^{9} \mathrm{z_j}\frac{\partial f(y_i, t, C_{\mathrm{fsh}})}{\partial y_i} = f(y_i, z_i, t, C_{\mathrm{fsh}}) \tag{20}$$

$$H = \sum_{i=1}^{9} z_i f(y_i, t, C_{\mathrm{fsh}}) \tag{21}$$

$$\left|\frac{dH}{dC_{\mathrm{fsh}}}\right|_t = 0 \tag{22}$$

The system of equations are solved stepwise, beginning with the state equations, which are integrated in the forward direction from starting time t_0 till the end of

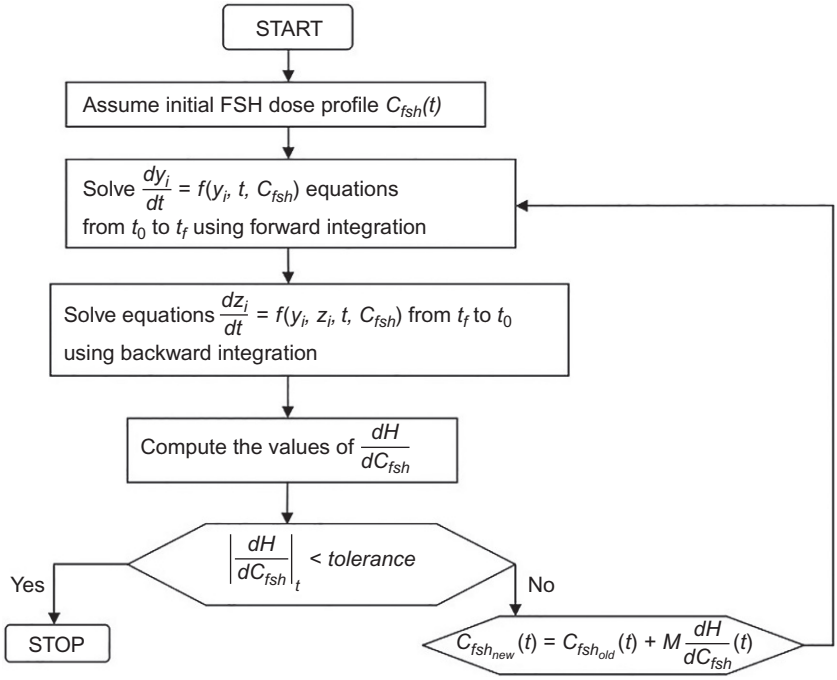

Fig. 6 Flowchart for optimal FSH dosage evaluation using the maximum principle.

the process or final time t_f. After this, the adjoint equations are integrated in the backward direction. Also, the optimality condition (Eq. 22) needs to be satisfied at every time point. The details of the calculation procedure are shown in the flowchart in Fig. 6.

3.3 Results from optimal control

As stated earlier, for days 1–4 the same dose is used, and no testing is done till 5th day. The optimal control method is applied to find dosage from 5th day onwards using the maximum principle. The patient parameters estimated using the two-day data are used, and the maximum principle method is applied to determine dosage from 5th day onwards. The optimal drug dosages for each patient are calculated, based on the starting dose, cycle days, and the initial FSD observed in each patient. The final-day mature follicle count using optimal control is then compared with observed mature follicles using the dosage specified by the attending physician for these 49 patients. Since the parameters from all-day data are more accurate than two-day data, those parameters are used with optimal control profile predicted by the two-day data for comparison. Fig. 7 shows the mature follicle distribution optimal versus experimental in Fig. 7A and the optimal dosage versus experimental dosage in Fig. 7B. The cumulative dose for this patient is found to be 2662.5 IU compared to

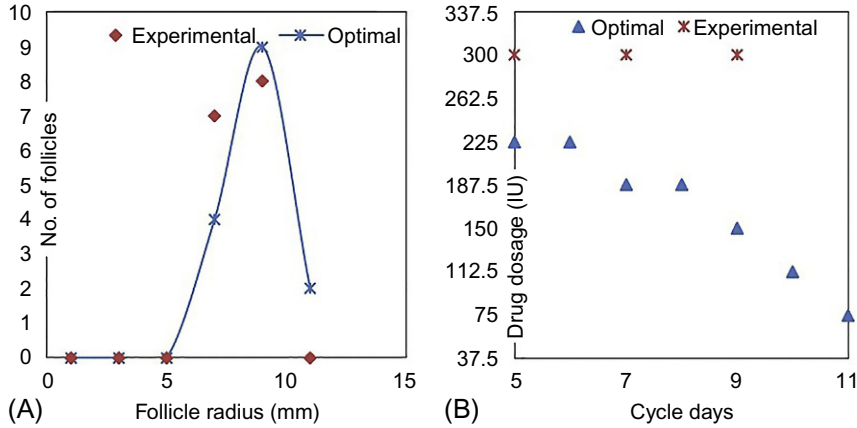

Fig. 7 (A) Follicular distribution for patient 3 predicted by optimal control with two-day parameters for the next day of the cycle versus observed follicle distribution from experiments for the last day of the cycle. (b) Optimal dosage for patient 3 predicted by optimal control with two-day parameters versus experimental dosage prescribed by doctor.

doctor prescribed dose of 3600 IU. The results serve as an example of the significant reduction in a dosage, which consequently reduces the costs to the patient.

The optimal control profile was calculated and customized for each patient for the clinical data available on 49 patient cycles. The histograms of the results are presented in Fig. 8. Fig. 8A shows the histogram of the ratio of optimal mature follicles to mature follicles observed using physician suggested dosage. Fig. 8B shows the % of reduction in dosage for each patient. It has been found that 98% of the patients show higher

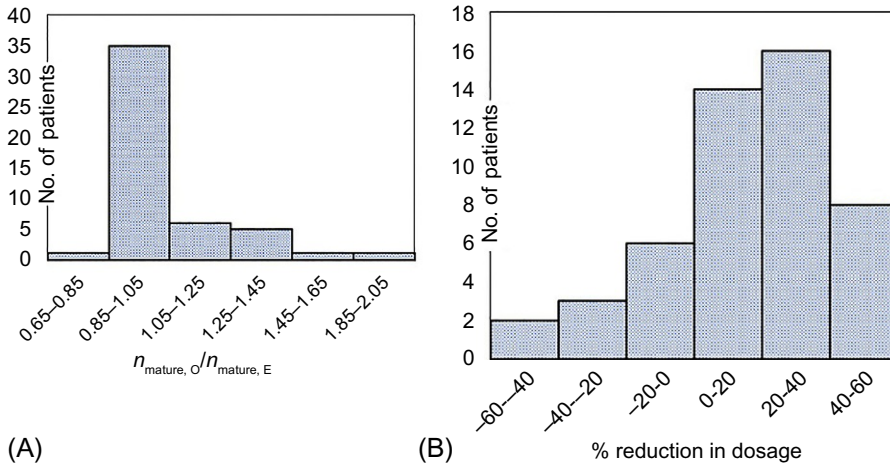

Fig. 8 Histogram of all patients: (A) Ratio of optimal mature follicles to experimental mature follicles. (B) % reduction in dosage.

mature follicles for the optimal control profile than the physician specified dosage. Most of these patients also show a significant reduction in dose requirements for successful superovulation. This also shows that the two-day data are sufficient to predict the optimal dosage for each patient.

Typically, older patients (age $>$ 35 years) are prescribed dosages on the higher side ranging from 300 to 450 IU. Even for the higher age for patient 3 (40 years), the results show that the actual dose needed to get similar outcomes is much less than as prescribed. Also, the starting doses are lower at 300 IU and 225 IU, thus corroborating the idea that lower starting doses can also achieve similar responses in patients. This study found no correlation between the age of patients and higher doses of 300–450 IU.

4 Overall approach for customized medicine

The model and optimal control methods are implemented in integrated software for clinical trials. This software is called OPTIVF (Diwekar, 2018). The software uses the initial two-day data from the patient, i.e., their FSD and hormone dosage, as an input to the model. Optimization-based parameter estimation (iterative) of the moment model described in Section 2 is carried out to customize the model for each patient. The parameters then are used along with the iterative optimal control capability to find optimal drug-dosing profile for the remaining days of the cycle. Fig. 9 shows a schematic of this procedure. Thus, daily tests are avoided, and a reduced amount of drugs can be used to obtain significantly better outcomes.

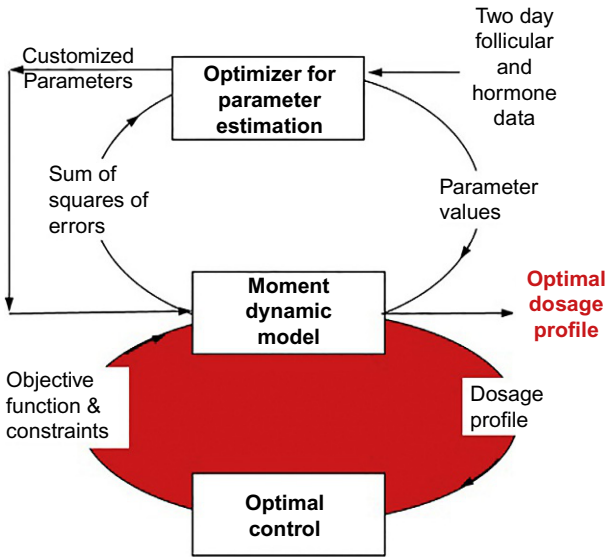

Fig. 9 Schematic of the overall approach and the steps in the OPTIVF software package.

4.1 Clinical trial using the software

Recently, the first clinical trial was conducted in Jijamata Hospital, Nanded. The trial involved 10 patients and was a double-blinded trial. Half of the patients were given dosage by the attending physician, and the other half were given the dosage predicted using this new approach using OPTIVF. Table 5 and Fig. 10 show the outcome for one of the patients in the clinical trial. Using the model and the optimized dosage, the follicular distribution at the end of the cycle in a clinical trial for this patient, it has been observed that the dosage predicted by using the model is 40 % less than that suggested by the IVF doctors (Fig. 10 and Table 5). Table 5 also shows that the number of mature follicles obtained at the end of the cycle using the model predicted dosage is significantly higher than that of physician suggested dosage. Percentage of good-quality eggs were similar from both the procedures. These results

Table 5 Comparison of optimal dosage profile with actual profile for patient 6

Patient 6	FSH Dr. Recom.	FSH optimal	No. of mature follicles on day 11 $9 \leq r \leq 12$		% of reduction in FSH due to optimization	% of reduction in testing due to optimization
Base follicle count -11	1950	1162.5	5 Dr. reco	11 (opt) actual follicles obtained	40.4%	72%

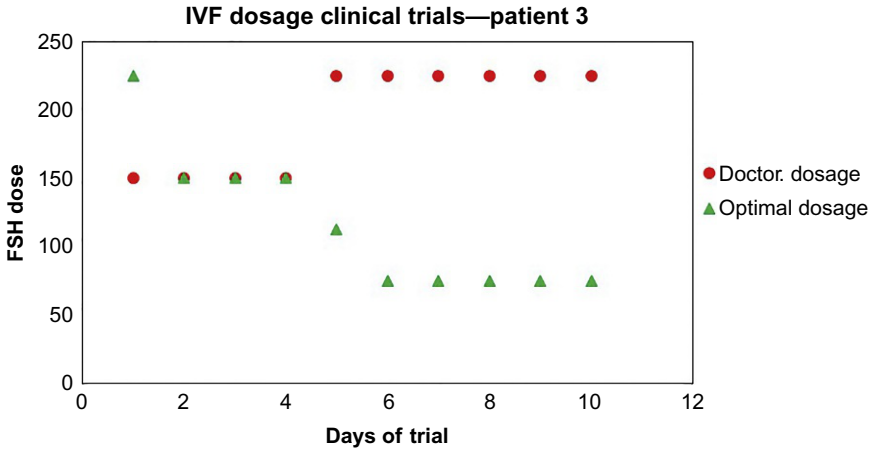

Fig. 10 Clinical trial patient 3, customized dosage comparison.

were consistent with all patients in this clinical trial. The testing requirement for patients using the optimized drug-dosage policy predicted by OPTIVF is reduced by 72%, and the number of follicles obtained was more than twice the number obtained by physician predicted dosage.

5 Summary and future work

IVF is the most common technique in assisted reproductive technology. Superovulation is a drug-induced method to enable multiple ovulation per menstrual cycle. The success of IVF depends upon successful superovulation, defined by the number and the uniformly high-quality of eggs retrieved in a cycle. Currently, this step is executed using almost daily monitoring of the follicular development using ultrasound and blood test. The daily dosage of hormones is customized for each patient based on these tests. Although there are general guidelines for the dosage, the dose is not optimized for each patient. The cost of testing and drugs makes this stage very expensive. To overcome the shortcoming of this system, a computer-assisted approach was presented for customized medicine for IVF. The approach uses customized models for each patient based on initial two-day data from each patient to determine the outcomes. Optimal control methods are then used on these customized models to obtain drug-dosage profiles for each patient. It has been found that this procedure provides better outcomes in terms of a higher number of mature follicles, reduced dosage, and reduced testing. This can reduce the side effects of the drugs significantly. A small clinical trial supports these theoretical findings. A user-friendly software was developed, which can provide a customized model of this stage for each patient, which would provide a basis for predicting the possible outcome based on the optimal drug-dosage profiles predicted by the optimal control functionality in the software. Further work is being carried out with the doctors in the United States to extend this approach to other protocols and for patients in the United States.

References

Allegra, A., Marino, A., Volpes, A., Coffaro, F., Scaglione, P., Gullo, S., La Marca, A., 2017. A randomized controlled trial investigating the use of a predictive nomogram for the selection of the FSH starting dose in IVF/ICSI cycles. Reprod. Biomed. Online 34, 429–438. https://doi.org/10.1016/j.rbmo.2017.01.012.

Alper, M.M., Smith, L.P., Sills, E.S., 2009. Ovarian hyperstimulation syndrome: current views on pathophysiology, risk factors, prevention, and management. J. Exp. Clin. Assist. Reprod. 6.

Baird, D.T., 1987. A model for follicular selection and ovulation: lessons from superovulation. J. Steroid Biochem. 27, 15–23.

Castiglione, F., Piccoli, B., 2007. Cancer immunotherapy, mathematical modeling and optimal control. J. Theor. Biol. 247, 723–732. https://doi.org/10.1016/j.jtbi.2007.04.003.

Czako, B., Sápi, J., Kovács, L., 2017. Model-based optimal control method for cancer treatment using model predictive control and robust fixed point method. In: 2017 IEEE 21st International Conference on Intelligent Engineering Systems (INES). Presented at the 2017 IEEE 21st International Conference on Intelligent Engineering Systems (INES), pp. 000271–000276. https://doi.org/10.1109/INES.2017.8118569.

Devroey, P., Tournaye, H., Van Steirteghem, A., Hendrix, P., Out, H.J., 1998. The use of a 100 IU starting dose of recombinant follicle stimulating hormone (Puregon) in in vitro fertilization. Hum. Reprod. 13, 565–566. https://doi.org/10.1093/humrep/13.3.565.

Diwekar, U., 2008. Introduction to applied optimization. In: Springer Optimization and Its Applications, second ed. Springer, New York.

Diwekar, U., 2018. OPTIVF: A User-Friendly Software for Optimization of IVF Cycles. Stochastic Research Technologies, LLC.

Dorn, C., 2005. FSH: what is the highest dose for ovarian stimulation that makes sense on an evidence-based level? Reprod. Biomed. Online 11, 555–561. https://doi.org/10.1016/S1472-6483(10)61163-7.

FastStats, 2018. https://www.cdc.gov/nchs/fastats/infertility.htm ((Accessed 3 March 2019)).

Fleming, R., Seifer, D.B., Frattarelli, J.L., Ruman, J., 2015. Assessing ovarian response: antral follicle count versus anti-Müllerian hormone. Reprod. Biomed. Online 31, 486–496. https://doi.org/10.1016/j.rbmo.2015.06.015.

Flood, A.E., 2002. Thoughts on recovering particle size distributions from the moment form of the population balance. Dev. Chem. Eng. Miner. Process. 10, 501–519. https://doi.org/10.1002/apj.5500100605.

Fritz, M.A., Speroff, L., 2010. Clinical Gynecologic Endocrinology and Infertility, eighth ed. LWW, Philadelphia.

Gordon, R., 2012. In Vitro Fertilization: ivf Process: And Embryo Transfer (IVF – ET). https://infofru.com/health/pregnancy/infertility-management-recent-advancement/in-vitro-fertilization-and-embryotransfer-ivf-et/ (Accessed 25 July 2019).

Hill, P., 2005. Batch crystallization. In: Korovessi, E., Linninger, A.A. (Eds.), Batch Processes. Taylor and Francis, CRC Press, New York, USA.

Hu, Q., Rohani, S., Jutan, A., 2005. Modelling and optimization of seeded batch crystallizers. Comput. Chem. Eng. Control Multiscale Distrib. Process Syst. 29, 911–918. https://doi.org/10.1016/j.compchemeng.2004.09.011.

John, V., Angelov, I., Öncül, A.A., Thévenin, D., 2007. Techniques for the reconstruction of a distribution from a finite number of its moments. Chem. Eng. Sci. 62, 2890–2904. https://doi.org/10.1016/j.ces.2007.02.041.

Jungheim, E.S., Meyer, M.F., Broughton, D.E., 2015. Best practices for controlled ovarian stimulation in in vitro fertilization. Semin. Reprod. Med. 33, 77–82. https://doi.org/10.1055/s-0035-1546424.

Khalili, S., Armaou, A., 2008. Sensitivity analysis of HIV infection response to treatment via stochastic modeling. Chem. Eng. Sci., Control Particul. Process. 63, 1330–1341. https://doi.org/10.1016/j.ces.2007.07.072.

Klemetti, R., Sevón, T., Gissler, M., Hemminki, E., 2005. Complications of IVF and ovulation induction. Hum. Reprod. 20, 3293–3300. https://doi.org/10.1093/humrep/dei253.

Kotanidis, L., Nikolettos, K., Petousis, S., Asimakopoulos, B., Chatzimitrou, E., Kolios, G., Nikolettos, N., 2016. The use of serum anti-Mullerian hormone (AMH) levels and antral follicle count (AFC) to predict the number of oocytes collected and availability of embryos for cryopreservation in IVF. J. Endocrinol. Invest. 39, 1459–1464. https://doi.org/10.1007/s40618-016-0521-x.

La Marca, A., Grisendi, V., Giulini, S., Argento, C., Tirelli, A., Dondi, G., Papaleo, E., Volpe, A., 2013. Individualization of the FSH starting dose in IVF/ICSI cycles using the antral follicle count. J. Ovarian Res. 6, 11. https://doi.org/10.1186/1757-2215-6-11.

La Marca, A., Sunkara, S.K., 2014. Individualization of controlled ovarian stimulation in IVF using ovarian reserve markers: from theory to practice. Hum. Reprod. Update 20, 124–140. https://doi.org/10.1093/humupd/dmt037.

Mascarenhas, M.N., Flaxman, S.R., Boerma, T., Vanderpoel, S., Stevens, G.A., 2012. National, regional, and global trends in infertility prevalence since 1990: A systematic analysis of 277 health surveys. PLoS Med. 9. https://doi.org/10.1371/journal.pmed.1001356.

Moon, K.Y., Kim, H., Lee, J.Y., Lee, J.R., Jee, B.C., Suh, C.S., Kim, K.C., Lee, W.D., Lim, J.H., Kim, S.H., 2016. Nomogram to predict the number of oocytes retrieved in controlled ovarian stimulation. Clin. Exp. Reprod. Med. 43, 112–118. https://doi.org/10.5653/cerm.2016.43.2.112.

Nisal, A., Diwekar, U., Bhalerao, V., 2019. Personalized medicine for in vitro fertilization procedure using modeling and optimal control. J. Theor. Biol. (accepted).

Randolph, A.D., 1988. Theory of Particulate Processes: Analysis and Techniques of Continuous Crystallization. Academic Press.

Nyboe Andersen, A., Nelson, S.M., Fauser, B.C.J.M., García-Velasco, J.A., Klein, B.M., Arce, J.-C., Tournaye, H., De Sutter, P., Decleer, W., Petracco, A., Borges, E., Barbosa, C.P., Havelock, J., Claman, P., Yuzpe, A., Višnová, H., Ventruba, P., Uher, P., Mrazek, M., Andersen, A.N., Knudsen, U.B., Dewailly, D., Leveque, A.G., La Marca, A., Papaleo, E., Kuczynski, W., Kozioł, K., Anshina, M., Zazerskaya, I., Gzgzyan, A., Bulychova, E., Verdú, V., Barri, P., García-Velasco, J.A., Fernández-Sánchez, M., Martin, F.S., Bosch, E., Serna, J., Castillon, G., Bernabeu, R., Ferrando, M., Lavery, S., Gaudoin, M., Nelson, S.M., Fauser, B.C.J.M., Klein, B.M., Helmgaard, L., Mannaerts, B., Arce, J.-C., 2017. Individualized versus conventional ovarian stimulation for in vitro fertilization: a multicenter, randomized, controlled, assessor-blinded, phase 3 noninferiority trial. Fertil. Steril. 107. https://doi.org/10.1016/j.fertnstert.2016.10.033. 387–396.e4.

Practice Committee of the American Society for Reproductive Medicine, 2018. Comparison of pregnancy rates for poor responders using IVF with mild ovarian stimulation versus conventional IVF: a guideline. Fertil. Steril. 109 (6), 993–999.

Rombauts, L., 2007. Is there a recommended maximum starting dose of FSH in IVF? J. Assist. Reprod. Genet. 24, 343–349. https://doi.org/10.1007/s10815-007-9134-9.

Scoccia, H., 2017. IVF Program Protocols for Assisted Reproductive Technologies. University of Illinois at Chicago.

Sighinolfi, G., Grisendi, V., La Marca, A., 2017. How to personalize ovarian stimulation in clinical practice. J. Turk. Ger. Gynecol. Assoc. 18, 148–153. https://doi.org/10.4274/jtgga.2017.0058.

Simopoulou, M., Sfakianoudis, K., Antoniou, N., Maziotis, E., Rapani, A., Bakas, P., Anifandis, G., Kalampokas, T., Bolaris, S., Pantou, A., Pantos, K., Koutsilieris, M., 2018. Making IVF more effective through the evolution of prediction models: is prognosis the missing piece of the puzzle? Syst. Biol. Reprod. Med. 64, 305–323. https://doi.org/10.1080/19396368.2018.1504347.

Sunderam, S., Kissin, D.M., Crawford, S.B., Folger, S.G., Boulet, S.L., Warner, L., Barfield, W.D., 2018. Assisted reproductive technology surveillance—United States, 2015. MMWR Surveill. Summ. 67, 1–28. https://doi.org/10.15585/mmwr.ss6703a1.

Ulas Acikgoz, S., Diwekar, U.M., 2010. Blood glucose regulation with stochastic optimal control for insulin-dependent diabetic patients. Chem. Eng. Sci. 65, 1227–1236. https://doi.org/10.1016/j.ces.2009.09.077.

van Tilborg, T.C., Torrance, H.L., Oudshoorn, S.C., Eijkemans, M.J.C., Koks, C.A.M., Verhoeve, H.R., Nap, A.W., Scheffer, G.J., Manger, A.P., Schoot, B.C., Sluijmer, A.V., Verhoeff, A., Groen, H., Laven, J.S.E., Mol, B.W.J., Broekmans, F.J.M., 2017. Individualized versus standard FSH dosing in women starting IVF/ICSI: an RCT. Part 1. The predicted poor responder. Hum. Reprod. 32, 2496–2505. https://doi.org/10.1093/humrep/dex318.

Yenkie, K.M., Diwekar, U., 2014. Optimal control for predicting customized drug dosage for superovulation stage of in vitro fertilization. J. Theor. Biol. 355, 219–228. https://doi.org/10.1016/j.jtbi.2014.04.013.

Yenkie, K.M., Diwekar, U., 2012. Stochastic optimal control of seeded batch crystallizer applying the ito process. Ind. Eng. Chem. Res. 52, 108–122.

Yenkie, K.M., Diwekar, U.M., Bhalerao, V., 2013. Modeling the superovulation stage in in vitro fertilization. IEEE Trans. Biomed. Eng. 60, 3003–3008.

Youssef, M.A., van Wely, M., Al-Inany, H., Madani, T., Jahangiri, N., Khodabakhshi, S., Alhalabi, M., Akhondi, M., Ansaripour, S., Tokhmechy, R., Zarandi, L., Rizk, A., El-Mohamedy, M., Shaeer, E., Khattab, M., Mochtar, M.H., van der Veen, F., 2016. A mild ovarian stimulation strategy in women with poor ovarian reserve undergoing IVF: a multicenter randomized non-inferiority trial. Hum. Reprod. https://doi.org/10.1093/humrep/dew282.

Yovich, J.L., Alsbjerg, B., Conceicao, J.L., Hinchliffe, P.M., Keane, K.N., 2016. PIVET rFSH dosing algorithms for individualized controlled ovarian stimulation enables optimized pregnancy productivity rates and avoidance of ovarian hyperstimulation syndrome. Drug Des. Devel. Ther. 10, 2561–2573. https://doi.org/10.2147/DDDT.S104104.

Control Applications for Biomedical Engineering Systems

Edited by Ahmad Taher Azar

Medical devices and sensors are routinely used to record various physiological signals for simple monitoring of human health, and sensing is an integral part of health monitoring. However, more advanced devices, signal measurement, modeling, and closed-loop control may be critical for surgical procedures, earlier diagnosis of diseases and disorders, drug administration, and clinical rehabilitation.

Control Applications for Biomedical Engineering Systems presents different control engineering and modeling applications in the biomedical field. It is intended for senior undergraduate or graduate students in both control engineering and biomedical engineering programs. For control engineering students, it presents the application of various techniques already learned in theoretical lectures, in the biomedical arena. For biomedical engineering students, it presents solutions to various problems in the field using methods commonly used by control engineers.

Ahmad Azar is a research associate professor at Prince Sultan University, Riyadh, Saudi Arabia. He is also an associate professor at the Faculty of Computers and Artificial intelligence, Benha University, Egypt.

Prof. Azar is the editor-in-chief of the *International Journal of System Dynamics Applications* (IJSDA) and the *International Journal of Service Science, Management, Engineering, and Technology* (IJSSMET) published by IGI Global, United States. Also, he is the editor-in-chief of the *International Journal of Intelligent Engineering Informatics* (IJIEI), Inderscience Publishers, Olney, United Kingdom. Prof. Azar has worked as Associate Editor of the *IEEE Transactions on Neural Networks* and *Learning Systems* from 2013 to 2017. He is currently Associate Editor of *ISA Transactions* (Elsevier) and IEEE Systems Journal. Prof. Azar has worked in the areas of control theory and applications, robotics, artificial intelligence, machine learning, and computational intelligence. He has authored/coauthored over 300 research publications in peer-reviewed reputed journals, book chapters, and conference proceedings.

Technology and Engineering / Mechanical

ISBN 978-0-12-817461-6

9 780128 174616

ELSEVIER

ACADEMIC PRESS

An imprint of Elsevier

elsevier.com/books-and-journals